

# On phase kinks, negative frequencies, and other third-order peculiarities of modulated surface waves

By IGOR SHUGAN AND KONSTANTIN VOLIAK

General Physics Institute, Russian Academy of Sciences, Moscow 117942, Russia

(Received 30 July 1997 and in revised form 17 March 1998)

Numerous laboratory and field experiments on nonlinear surface wave trains propagating in deep water (Lake & Yuen 1978; Ramamonjjarisoa & Mollo-Christensen 1979; Mollo-Christensen & Ramamonjjarisoa 1982; Melville 1983) have showed a specific wave modulation that so far has not been explained by nonlinear theories. Typical effects were the so-called wave phase reversals, negative frequencies, and crest pairing, experimentally observed in some portions of the modulated wave train. In the present paper, in order to explain these modulation manifestations, the equations for wavenumber, frequency, and velocity potential amplitude are derived consistently in the third-order approximation related to the wave steepness. The resulting model generalizes, for instance, the well-known nonlinear Schrödinger equation theory, to which it transforms at certain values of the governing parameters.

The stationary solutions to the derived set of equations are found in quadrature and then analysed. Within well-defined ranges of the model parameters, these solutions explicitly manifest the above-mentioned wave modulation effects. In particular, they show the wave phase kinks to arise on areas of relatively small free-surface displacement in complete accord with the experiments.

The model with deeply modulated wavenumber and frequency permits one also to analyse the appropriately short surface wavepackets and modulation periods. In this case, a variety of new interesting wave solutions arises revealing complicated alteration of smooth and rough portions of the free surface. Of special importance are solitary waves, naturally generalizing envelope solitons of the nonlinear Schrödinger equation, but having a varying frequency (as a principle of the proposed theory) and a non-zero wave ‘pedestal’ at infinity. These new types of modulated surface waves should be also observable in laboratory tanks and under field conditions, because the relevant free parameters of theory are not extreme.

---

## 1. Introduction

For the past two decades experiments on the nonlinear wave propagation on water surfaces have revealed a number of modulation effects that have not been explained by theorists. Lake & Yuen (1978) were the first who observed the wave crests ‘lost’ at a quasi-zero amplitude (node) of deeply modulated surface wave trains. Then a similar effect was found by Ramamonjjarisoa & Mollo-Christensen (1979) and Mollo-Christensen & Ramamonjjarisoa (1982) in wind sea waves and under laboratory conditions: a nonlinear surface wave merged with the foregoing one and then disappeared. As a result of such a ‘crest pairing’, the wave period is doubled

instantaneously. These local effects in the wave field are sometimes assumed to be responsible for a long-fetch downshift (Huang, Long & Shen 1996) of the average wave frequency.

Melville (1983) investigated thoroughly the evolution of an initially uniform train of Stokes surface waves in a long laboratory tank. At the wave fetch beginning, he observed the development of the well-known Benjamin–Feir (1967) sideband instability resulting in weak amplitude–frequency modulation of the wave train. As nonlinear effects accumulated along the tank, an asymmetry arose in the wave envelope related to its maximum. The relative phase between modulations of wave amplitude and frequency also changed: the initial phase lag of  $\frac{1}{2}\pi$  tended to  $\pi$  and, in the developed nonlinear mode, the amplitude was modulated with phase opposite to that of frequency modulation. At a longer distance, Melville observed the most prominent features of that mode, the so-called phase ‘reversals’ accompanied by very large variations in the wavenumber, frequency, and phase velocity. In particular, the frequency turned out even to be negative near those local phase kinks.

Observing the drastic modulational development of nonlinear wave groups, Chere-skin & Mollo-Christensen (1985) after an elaborate numerical study stated it to be impossible to describe these effects with the use of the nonlinear Schrödinger equation (NSE) derived by Zakharov (1968) as well as of any weakly nonlinear (third-order) theory. According to the NSE theory, an initially uniform wave train propagates periodically transforming into a coupled group of envelope solitons and vice versa (Zakharov & Shabat 1972). The NSE model has often been improved to describe more adequately various regimes of finite-amplitude surface wave propaga-tion. The most popular in this field was the study of the wave self-interaction on the basis of more accurate modulational equations including the fourth-order terms in wave steepness (Roskes 1977; Dysthe 1979; Tomita 1986; Lo & Mei 1985, 1987; Akylas 1989, 1991). These works explained the so-called group splitting observed in deep-water experiments by Feir (1967) and Su (1982), when an initially symmetrical (NSE-type) surface wave group became an ordered sequence of packets after long-fetch propagation due to the average frequency downshift in leading packets. The proper downshift indicates that the theory may be enhanced by weakening restrictions imposed onto the wavepacket spectrum variation. In fact, the numerically integrated fourth-order NSE model applied to a bimodal wave spectrum yields quantitative agreement with experiments (Lo & Mei 1985; Stansberg 1995). Furthermore, that model with dissipation is in qualitative agreement with the experimentally observed frequency downshift (Hara & Mei 1991, 1994; Kato & Oikawa 1995; Uchiyama & Kawahara 1994). Unfortunately, numerical analyses of this kind do not explain the listed peculiarities of deeply modulated surface waves (phase kinks, negative frequencies, crest pairing).

The NSE deduced in the third-order approximation in wave steepness is always based on the principle of a spectrally narrow modulation. However, we believe that the general potency of the uniformly valid expansion in this approximation is not exhausted by known solutions found for the wave envelope within the NSE theory.

The main goal of the present paper is to derive and study a general set of the third-order equations for slowly modulated wave trains propagating on the surface of deep water. As distinct from other works, the proposed model should allow for a variety of uniformly valid solutions with the wavenumber and frequency having relative variations of the order of unity over the ‘slow’ coordinate and time. This deep wave modulation observed in the above-mentioned experiments is not described by the classical NSE theory. In this work an asymptotic two-scale expansion will be applied

directly to the velocity potential and free-surface displacement of irrotational water motion. The subsequent stationary solution to the modulational equations derived for three functions characterizing the motion (the potential amplitude, wavenumber, and frequency) should give a uniformly valid asymptotics for weakly nonlinear surface waves to describe the wave phase reversals and other deep modulation effects. It is noteworthy that the equations to be solved are similar in essence to those written by Chu & Mei (1970, 1971) and are analysed here to take substantially deep modulation into account.

The theory presented should reduce to the NSE model at certain values of the controlling parameters. However, we hope to discover in this way other special modes of wavepacket propagation, having the same origin as the above local phase kinks. For instance, it would also be interesting to find a generalization to the NSE envelope solitons in the form of solitary wavepackets with somewhat different properties.

The proposed account for deep modulation can extend the applicability range for modulational equations, for example, to model sufficiently short wavepackets. Usually these wave groups with no distinct envelope are described by combined equations with higher-order dispersion terms additional to the NSE-type ones involving nonlinear group velocity, wave aberration, etc. (see, for instance Gromov & Talanov 1996). We hope to show the NSE solitons to be merely a specific class of solitary solutions that can have a non-zero wave amplitude at infinity. In turn, these solitary waves exemplify more general modulated wave trains, to which the definition of a slowly varying envelope is hardly applicable.

The paper is organized in the following manner. Section 2 contains the problem's initial statement including its scaling and assumptions necessary to derive the governing modulational equations in partial derivatives for the first-order potential amplitude, wavenumber, and frequency. Restricted travelling surface wave solutions are found and qualitatively analysed in §3 with the use of the phase plane of potential and velocity amplitudes, depending on the fluxes of wave energy and action, as well as on the frequency detuning from group resonance. Various wave modulation regimes are exhibited and discussed in §4 by the examples of two lowest harmonics of the free-surface displacement, as well as by the wave frequency and phase. In §5 we present concluding remarks.

## 2. Main equations

The set of equations for potential motion of an ideal incompressible infinite-depth fluid with the free surface is given by:

the Laplace equation

$$\phi_{xx} + \phi_{zz} = 0, \quad -\infty < z < \eta(x, t), \quad (2.1)$$

the boundary conditions at the free surface

$$\phi_t + g\eta + \frac{1}{2}(\phi_x^2 + \phi_z^2) = 0, \quad z = \eta(x, t), \quad (2.2)$$

$$\eta_t + \phi_x \eta_x = \phi_z, \quad z = \eta(x, t), \quad (2.3)$$

and at the bottom

$$\phi = 0, \quad z = -\infty. \quad (2.4)$$

Here  $\phi(x, z, t)$  and  $\eta(x, t)$  are the velocity potential and the free-surface displacement,  $g$  is the gravity acceleration, and  $t$  is the time. Horizontal and vertical (in the upward

direction) axes of an orthogonal Cartesian coordinate frame are denoted as  $x$  and  $z$ , respectively.

Let us normalize the variables as follows:

$$\begin{aligned} \phi &= a_0 \left( \frac{g}{k_0} \right)^{1/2} \phi', & \phi' &= \epsilon \left( \frac{g}{k_0^3} \right)^{1/2} \phi', & \eta &= a_0 \eta' = \frac{\epsilon}{k_0} \eta', \\ t &= \frac{1}{(gk_0)^{1/2}} t', & z &= \frac{z'}{k_0}, & x &= \frac{x'}{k_0}, \end{aligned} \quad (2.5)$$

where  $a_0$  is a characteristic free-surface displacement,  $2\pi/k_0$  is a typical surface wavelength,  $\epsilon = a_0 k_0$  is the conventional average wave steepness parameter, and the dimensionless quantities are primed. It is noteworthy that normalization (2.5) explicitly specifies the principal scales of sought functions  $\phi = O(\epsilon)$  and  $\eta = O(\epsilon)$ . Then, the set (2.1)–(2.4) is reduced to the form

$$\phi_{xx} + \phi_{zz} = 0, \quad -\infty < z < \epsilon\eta(x, t), \quad (2.6)$$

$$-\eta = \phi_t + \frac{1}{2} \epsilon (\phi_x^2 + \phi_z^2), \quad z = \epsilon\eta(x, t), \quad (2.7)$$

$$\eta_t + \epsilon \phi_x \eta_x = \phi_z, \quad z = \epsilon\eta(x, t), \quad (2.8)$$

$$\phi = 0, \quad z = -\infty, \quad (2.9)$$

where the primes are omitted. Further analysis is based on the assumption of small parameter  $\epsilon \ll 1$ ; therefore the weakly nonlinear surface wave train is described by a solution to equations (2.6)–(2.9), expanded into a Stokes series in terms of  $\epsilon$ .

Assuming also the wave motion phase  $\theta = \theta(x, t)$ , we define the wavenumber and frequency in the usual way as

$$k = \theta_x, \quad \omega = -\theta_t. \quad (2.10)$$

These main wave parameters together with the first-order velocity potential amplitude  $\phi_0$  will be considered further as slowly varying with the characteristic scale  $O(\epsilon^{-1})$  longer than the primary wavelength and period (Chu & Mei 1970):

$$\phi_0 = \phi_0(\epsilon x, \epsilon t), \quad k = k(\epsilon x, \epsilon t), \quad \omega = \omega(\epsilon x, \epsilon t). \quad (2.11)$$

On this basis we attempt to recover the effects of nonlinear wave dispersion additional (having the same order) to Stokes' (1849) term with the wave steepness squared.

The solution to the problem, uniformly valid to  $O(\epsilon^3)$ , is found by a two-scale expansion with the differentiation

$$\frac{\partial}{\partial t} = -\omega \frac{\partial}{\partial \theta} + \epsilon \frac{\partial}{\partial T}, \quad \frac{\partial}{\partial x} = k \frac{\partial}{\partial \theta} + \epsilon \frac{\partial}{\partial X}, \quad T = \epsilon t, \quad X = \epsilon x. \quad (2.12)$$

We search for the velocity potential  $\phi = \phi(x, z, t)$  satisfying the Laplace equation (2.6) up to  $O(\epsilon^2)$ ,

$$\phi = \phi_0 e^{kz} \sin \theta + \epsilon (\gamma z + \delta z^2) e^{kz} \cos \theta + \dots, \quad (2.13)$$

where  $\phi_0$ ,  $\gamma$ , and  $\delta$  are the functions of  $O(\epsilon)$  to be determined in 'slow' variables  $X$  and  $T$ , while  $k = O(1)$ .

The second (absolute)-order term appears in (2.13) as an unusual parabolic-profile jet  $\gamma z + \delta z^2$  oscillating with the fundamental wave phase  $\theta$ . (The second-harmonic potential is omitted since it gives rise only to  $O(\epsilon^4)$  corrections to satisfy the boundary conditions.) However, Yuen & Lake (1975) had employed a profile of the oscillatory subsurface current linear in  $z$ . This jet is caused by the modulated wavenumber distorting the conventional exponential decay of surface waves with depth. Obviously

expansion (2.13) is not unique, but all possible expansions of the fluid velocity potential (and the free-surface displacement) should be equivalent within the accepted accuracy for the modulated wavenumber and frequency.

One sees also that an induced zero-harmonic potential  $\bar{\phi}$  of  $O(\epsilon^2)$  (see Dysthe 1979; Lo & Mei 1985) is not included in (2.13), because the pair of functions  $\bar{\phi}, \bar{\eta}$  (where the latter is the relevant induced displacement) arise in the modulational equations only in terms of  $O(\epsilon^4)$ . Analogously, we take no account of the potential  $O(\epsilon^3)$  terms since these are balanced in the linear parts of boundary conditions (2.7) and (2.8) and do not change the third-order modulation equations.

Substituting potential (2.13) into the Laplace equation (2.6) and equating the coefficients at the same orders in  $\epsilon$ , we find directly the modulational corrections to the vertical velocity profile

$$\gamma = -\phi_{0X}, \quad \delta = -\frac{1}{2} k_X \phi_0. \quad (2.14)$$

The free-surface displacement  $\eta = \eta(x, t)$  is also sought as an asymptotic series,

$$\eta = \eta_0 + \epsilon \eta_1 + \epsilon^2 \eta_2 + \dots, \quad (2.15)$$

where  $\eta_0, \eta_1$ , and  $\eta_2$  are  $O(\epsilon)$  functions of  $X$  and  $T$ . Using expressions (2.13)–(2.15) subject to the dynamic boundary condition (2.7), we find the components of the free-surface displacement

$$\eta_0 = \omega \phi_0 \cos \theta, \quad (2.16)$$

$$\eta_1 = -\phi_{0T} \sin \theta + \frac{1}{2} \omega^2 k \phi_0^2 \cos 2\theta - \frac{1}{2} k(k - \omega^2) \phi_0^2, \quad (2.17)$$

$$\eta_2 = -\frac{3}{8} \omega k^3 \phi_0^3 \cos \theta + \dots \quad (2.18)$$

The first term in (2.17) has the fundamental frequency shifted in phase from (2.16) due to the time-dependent potential (cf. Yuen & Lake 1975), while the third one is of  $O(\epsilon^4)$  as induced by nonlinear deflection  $k - \omega^2$  from the dispersion relation for infinitesimal waves and should be neglected. Only the self-action term with fundamental wave phase  $\theta$  is included in the third-order displacement (2.18).

Substitution of velocity potential (2.13)–(2.14) and surface displacement (2.16)–(2.18) into the kinematic boundary condition (2.8) gives the following relationships between the wave modulation characteristics:

$$\omega^2 = k + \omega^2 k^3 \phi_0^2 + \phi_{0TT} / \phi_0, \quad (2.19)$$

$$(\omega \phi_0)_T + \omega \phi_{0T} + \phi_{0X} = 0. \quad (2.20)$$

The first of these formulas, representing the dispersion relation with the total second-order amplitude–phase dispersion included, simplifies to

$$\omega^2 = k + k^4 \phi_0^2 + \phi_{0TT} / \phi_0. \quad (2.21)$$

Equation (2.20) yields the known wave action conservation law

$$(\omega \phi_0^2)_T + \frac{1}{2} (\phi_0^2)_X = 0. \quad (2.22)$$

Modulational equations (2.21) and (2.22) are closed by the equation of wave phase conservation that follows from (2.10) as a compatibility condition

$$k_T + \omega_X = 0. \quad (2.23)$$

Closed set (2.21)–(2.23) defines all three unknown modulation functions: the first-order potential amplitude  $\phi_0$ , wavenumber  $k$ , and frequency  $\omega$ . These equations are mathematically (to an accepted order) equivalent to equations (7.1) derived by Chu

& Mei (1970) but compared to the latter the wave dispersion law (2.21) is not linearized by rooting. By derivation, the total frequency  $\omega$  contributes in the wave action law (2.22), while only the frequency linear part  $\omega_0$  was taken into account in Chu & Mei's equation (7.1). The resulting difference of  $O(\epsilon^4)$  is obviously beyond our consideration. In fact, the effects of nonlinear group velocity are introduced by an  $O(\epsilon^2)$  correction to the first term of (2.22), keeping the wave action to be invariant within the second order (Whitham 1974). The meaning of the term with twice differentiation in (2.21) was explained by Chu & Mei (1971) as the second-order effect of the modulation rate. However the most important point is that Chu & Mei (1970) in their equations for permanent waves assumed additionally  $c_g = c + O(\epsilon)$ , where  $c_g$  is the wave group velocity and  $c$  is the observer's velocity. In the present work we do not use such an assumption, setting  $c_g = c + O(1)$ . The corresponding relative variations in the wavenumber and frequency have also an order of unity. Even though the wave train remains narrowbanded around these instantaneous wave characteristics at all times and locations, the effective (for instance, experimentally measured) wave spectrum has a width determined just by these variations. Such a train will be hereafter referred to as deeply modulated.

### 3. Travelling wave solutions

Let us find travelling wave solutions to the problem (2.21)–(2.23), supposing all the unknown functions to depend on the single coordinate  $\xi = X - cT$ , where  $c$  is the velocity of a reference frame where the waves are stationary. It is noteworthy that the velocity  $c$  need be not high,  $c = O(1)$ , in order to keep the accepted scaling. Then, after integrating (2.23) and (2.24), the problem has the form

$$\omega^2 = k + k^4 \phi_0^2 + c^2 \phi_{0\xi\xi} / \phi_0, \quad (3.1)$$

$$(-c\omega + \frac{1}{2}) \phi_0^2 = A, \quad (3.2)$$

$$-ck + \omega = \Omega, \quad (3.3)$$

where  $A$  and  $\Omega$  are the integration free constants with obvious physical meaning of the wave action flux and frequency, respectively, measured in the laboratory coordinate frame.

After eliminating the wavenumber  $k$  and frequency  $\omega$  the set (3.1)–(3.3) transforms into a single equation for the first-order potential amplitude  $\phi_0$ . We renormalize the controlling constant  $A$ , unknown variable  $\phi_0(\xi)$ , and accompanying coordinate  $\xi$ , then introduce a laboratory frequency detuning  $\Delta$  from the group resonance by

$$A = c^6 \tilde{A}, \quad \phi_0 = c^3 \tilde{\phi}_0, \quad \xi = c^2 \tilde{\xi}, \quad \Delta = \frac{1}{2} - c\Omega. \quad (3.4)$$

Now, omitting tildes (or, equivalently, setting the observer's velocity to unity,  $c = 1$ ), we write down the main equation to be analysed:

$$\phi_{0\xi\xi} = \phi_0 \left( \frac{1}{2} - \frac{A}{\phi_0^2} \right)^2 - \phi_0 \left( \Delta - \frac{A}{\phi_0^2} \right) - \phi_0^3 \left( \Delta - \frac{A}{\phi_0^2} \right)^4. \quad (3.5)$$

We note at once that equation (3.5) has the exact first integral

$$\frac{1}{2} (\phi_{0\xi})^2 = -\frac{1}{4} \Delta^4 \phi_0^4 + \frac{1}{4} \frac{A^4}{\phi_0^4} + \frac{1}{2} \left( \frac{1}{4} - \Delta + 4\Delta^3 A \right) \phi_0^2 - \frac{1}{2} \frac{A^2 + 4\Delta A^3}{\phi_0^2} - 6\Delta^2 A^2 \ln \phi_0 + E, \quad (3.6)$$

where we assign the meaning of preserved wave energy flux, for instance, emitted by a

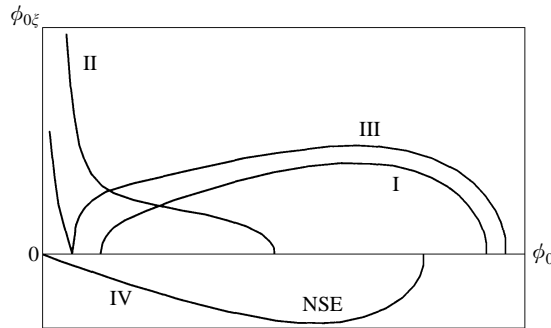


FIGURE 1. Typical phase trajectories of equation (3.5): periodic solution (I), when the right-hand side of (3.5) has two real roots; singular solution (II) not satisfying the model assumptions (relevant real roots are absent); intermediate solution (III) consisting of the integral curves of types I and II for the pair of coinciding roots; and classical NSE envelope soliton (IV) at zero fluxes of wave action,  $A = 0$ , and energy,  $E = 0$ .

source at  $\xi = -\infty$ , to the integration constant  $E$ . As a solution to the travelling wave problem, the first-order potential amplitude  $\phi_0$  is determined via (3.6) in quadrature.

The structure of this solution to equation (3.5) allows us to consider the phase plane (figure 1) in coordinates of horizontal velocity  $\phi_{0\xi}$  and potential amplitude  $\phi_0$ . There, the sought solutions form a three-parameter  $(A, E, \Delta)$  family with two main types of trajectories:

(i) closed type I curves (only the upper part of the curve is shown in figure 1, while the lower half is symmetrical with respect to the axis  $\phi_0$ ) that describe periodic functions  $\phi_0(\xi)$ , as well as  $k(\xi)$  and  $\omega(\xi)$ , for travelling surface waves with the extreme amplitudes corresponding to the edge points  $\phi_{0\min}$  and  $\phi_{0\max}$  of the plotted cycle; the proper potential  $\phi(\xi, z)$  and surface elevation  $\eta(\xi)$  are quasi-periodic along the cycle;

(ii) type II curves (also symmetrical with respect to the abscissa) which are singular at the point  $\phi_0 = 0$  with infinite horizontal velocities  $\phi_{0\xi} \rightarrow \infty$ . In the vicinity of the phase-plane centre the solution to (3.6) satisfies an asymptotic equation  $\frac{1}{2}\phi_{0\xi}^2 \approx \frac{1}{4}A^2/\phi_0^4$ . Hence the free-surface potential remains restricted there,  $\phi_0(\xi) \propto A^{2/3}\xi^{1/3}$ , while the wave frequency is singular,  $\omega(\xi) \propto \xi^{-2/3}$ , together with the free-surface displacement,  $\eta_0(\xi) = \omega\phi_0 \propto \xi^{-1/3}$ . Therefore, the main assumptions of restricted and slowly varying modulational functions are not met by the type II characteristics and these are beyond our consideration.

The integral cycles I of figure 1 are defined by two real roots of the equation

$$\phi_{0\xi\xi} = 0, \tag{3.7}$$

pointing to the existence of two extrema for the right-hand side of (3.6), which mean periodic modulation of the fluid velocity amplitude  $\phi_{0\xi}$  and thus the potential amplitude  $\phi_0$ . Only the type II singular trajectories exist formally at the absence of those extrema.

After excluding the trivial root  $\phi_0 = 0$ , equation (3.7) takes the form of the quartic equation in the squared variable  $\phi_0^2$  with two parameters  $\Delta$  and  $A$ ,

$$\frac{1}{4} - \Delta + \frac{A^2}{\phi_0^4} - \phi_0^2 \left( \Delta - \frac{A}{\phi_0^2} \right)^4 = 0. \tag{3.8}$$

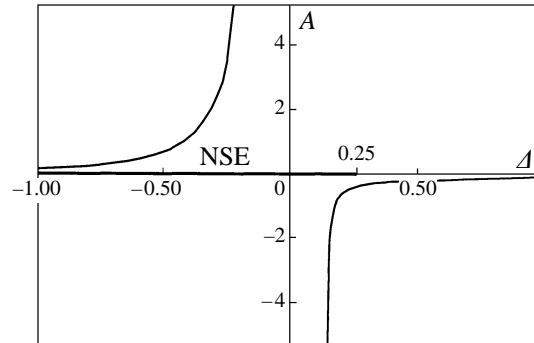


FIGURE 2. Region of existence (between the curves) of periodically and quasi-periodically modulated travelling waves in the coordinates of normalized wave action flux  $A$  and group detuning  $\Delta$ . The ray directed from the point  $\Delta = 1/4$  to the left along the abscissa axis displays the relevant region for the NSE solutions.

The real roots of equation (3.8), when

$$\phi_0^2 = \frac{A}{1/2 - c\omega} \geq 0, \quad (3.9)$$

correspond to the opposite directions (signs) of wave action flux  $A$ , related to the sign of detuning between the laboratory system velocity  $c$  and the wave group velocity  $(2\omega)^{-1}$ , which follows from definition (3.2). Then solving equation (3.8), we find that (3.7) has positive roots  $\phi_0^2$  (3.9), and thus equation (3.5) has periodic solutions in the region of parameters  $A$  and  $\Delta$  between the two curves plotted in figure 2.

The case of coalescing roots for (3.7), shown by two-branched trajectory III in figure 1 is intermediate between the wave motions of types I and II. The type III trajectories touch (cross) the  $\phi_0$ -axis at the point separating the type I modulational cycles and the type II singular solutions. This phase point corresponds to infinite physical coordinates  $\xi \rightarrow \pm\infty$ , thus forbidding transitions between these solution branches. Obviously, the cyclic branch corresponds to a 'bright' solitary wavepacket riding on the permanent wave background specified by the above separating point. Meantime the singular branch of curve III, infinitely growing near the phase-plane origin, might conceivably point to an existence of 'black' solitary (anti)packets suppressing totally the permanent wave train down to  $\phi_0 = 0$ . (Similar to the type II curves, this branch does not satisfy the initial assumptions.)

The bright solitary waves manifest conventional NSE dynamics at zero action flux  $A = 0$  (group resonance) and zero energy flux  $E = 0$ . In this case, the NSE envelope soliton arises as shown in figure 1 by the integral cycle IV. (Half of it is plotted in the fourth diagram quadrant.) Here the right-hand side of equation (3.5) is a cubic polynomial with the zero root  $\phi_0 = 0$  and the roots  $\phi_0 = \pm\Delta^{-2}(1/4 - \Delta)^{1/2}$  for group detuning  $\Delta \leq 1/4$ . Other travelling (cnoidal) NSE wave envelopes are controlled by the relationship between  $\Delta$  and  $E$ . The region of existence for the NSE wave solutions is marked in figure 2 by a ray directed from the point  $\Delta = 1/4$  to the left along the abscissa.

Noteworthy is the specific behaviour of modulated waves in the vicinity of a critical amplitude  $\phi_{0c} = (2A)^{1/2}$  not shown in figure 1 because all curves are plotted there for different  $A$ . If the modulation cycles cross this vertical line, then, by virtue of (3.2), some wave train portions are quasi-periodically suppressed at the free surface, because the frequency  $\omega$  together with the (principal part of) elevation  $\eta \propto \omega\phi_0$  tend



simultaneously to zero. The trajectories  $\phi_{0\xi} = \phi_{0\xi}(\phi_0)$  have no peculiarities at this critical point.

#### 4. Analysis of solutions and discussion

All properties of the restricted travelling wave solutions are analysed by integrating equation (3.6) in quadrature for various combinations of the three controlling parameters  $A$ ,  $A$ , and  $E$ . The most interesting stationary solutions are illustrated by the plots of modulation parameters: the reduced wave frequency

$$c\omega(\xi) = \frac{1}{2} - \frac{A}{\phi_0^2(\xi)} \quad (4.1)$$

and phase

$$c\theta(\xi) = \int_0^\xi \left[ \frac{1}{2} - \frac{A}{\phi_0^2(\xi')} \right] d\xi', \quad (4.2)$$

as well as by the profiles of two lowest harmonics of the free-surface displacement (see (2.16)–(2.18))

$$\eta^{(1)}(\xi) = \omega\phi_0 \cos \theta - c\phi_{0\xi} \sin \theta - \frac{3}{8}k^2\omega^3\phi_0^3 \cos \theta, \quad (4.3)$$

$$\eta^{(2)}(\xi) = \frac{1}{2}k\omega^2\phi_0^2 \cos 2\theta. \quad (4.4)$$

In all calculations the maximum or the minimum potential amplitudes at the points where the modulation cycle crosses the abscissa (see figure 1) are taken as ‘starting’  $\phi_0$  values.

##### 4.1. Positive wave action flux

Let us first consider using concrete examples the main properties of permanent-form periodic solutions for the positive wave action flux  $A > 0$ , when the wave group velocity exceeds the velocity of an observer,  $c_g = (2\omega)^{-1} > c$ . In this case, it follows from (4.1) that the instantaneous frequency is higher for larger wave amplitudes and differs from the maximum value  $\omega_{\max} = (2c)^{-1}$  by a quantity proportional to the action flux and inversely proportional to the amplitude squared. Thus as nonlinear effects grow quite slowly (quasi-stationarily) at a constant and positive wave action flux, one should observe a specific average frequency upshift in travelling surface waves.

At sufficiently large wave amplitudes, when  $\phi_0 > (2A)^{1/2}$ , the wave frequency increases as the amplitude grows and vice versa; therefore these functions can be modulated rather smoothly and almost in phase along the coordinate  $\xi$ . We will start our consideration from such a case resembling qualitatively the wave self-modulated solutions to the classical NSE equation. Figure 3 shows two lowest harmonics of the surface profile  $\eta(\xi)$  together with the reduced frequency  $c\omega(\xi)$  and phase  $c\theta(\xi)$  for the following wave parameters: action flux  $A = 0.30$ , group detuning  $\Delta = 0.22$ , energy flux  $E = 0$ , and average steepness  $\epsilon = 0.25$ . For better comparison, we reproduce the second-harmonic displacement  $\eta^{(2)}(\xi)$  on the same scale as the first harmonic  $\eta^{(1)}(\xi)$ . In this case of group resonance corresponding to a type I modulation loop in figure 1, the zero energy flux implies that there are no wave sources at infinity.

One sees from figure 3 that the wave system as a whole is modulated smoothly in a regular manner close to the NSE-type ‘cnoidal’ envelope because the first harmonic  $\eta^{(1)}$  noticeably exceeds the critical quantity  $\omega(2A)^{1/2} \approx 0.775\omega$  everywhere on the  $\xi$ -axis. In contrast to the fundamental harmonic, the second-harmonic elevation  $\eta^{(2)}$  has no

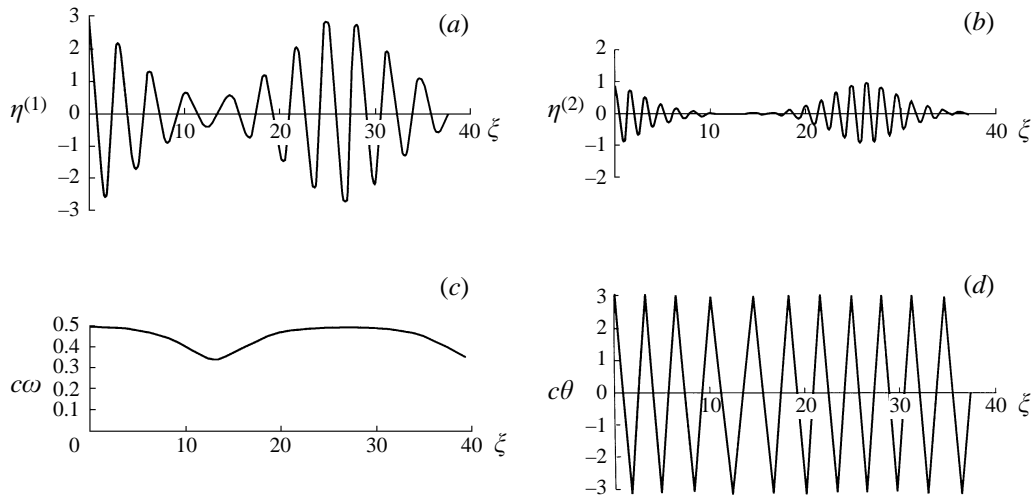


FIGURE 3. Normalized first (a) and second (b) harmonics of surface profile  $\eta(\xi)$ , wave frequency  $c\omega(\xi)$  (c), and phase  $c\theta(\xi)$  (d) for wave action flux  $A = 0.30$ , group detuning  $\Delta = 0.22$ , energy flux  $E = 0$ , and steepness  $\epsilon = 0.25$ ;  $c$  is the laboratory frame velocity.

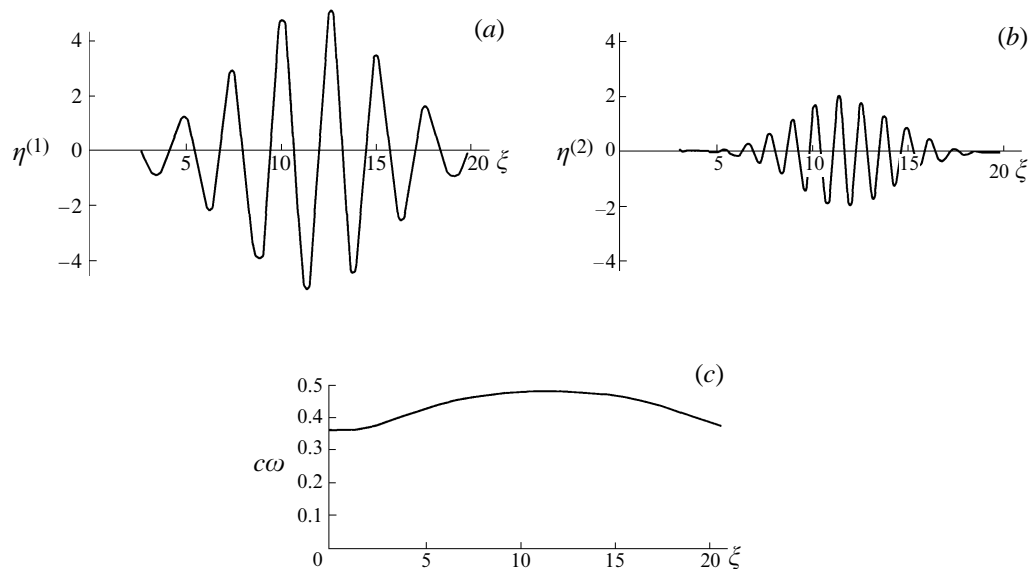


FIGURE 4. As figure 3 but with  $A = 0.92$ ,  $\Delta = 0.22$ ,  $E = 0.135$  and  $\epsilon = 0.235$ .

permanent component and is deeply modulated like a sequence of pulses. The wave frequency  $c\omega$  follows the wavepacket 'envelope' and the phase  $c\theta$  is almost linear in the coordinate  $\xi$ .

Retaining the same group detuning  $\Delta = 0.22$  as in figure 3 and the wave steepness  $\epsilon = 0.235$  close to the previous value, we choose the flux values  $A = 0.92$  and  $E = 0.135$ , so that the relevant type III trajectory would touch (cross) the abscissa as in figure 1 and the trajectory's cyclic branch would correspond to the solutions with an infinite period and a permanent wave motion at infinity. The relevant solitary wave group is shown in figure 4 as a perturbation of the permanent wave train. One sees here

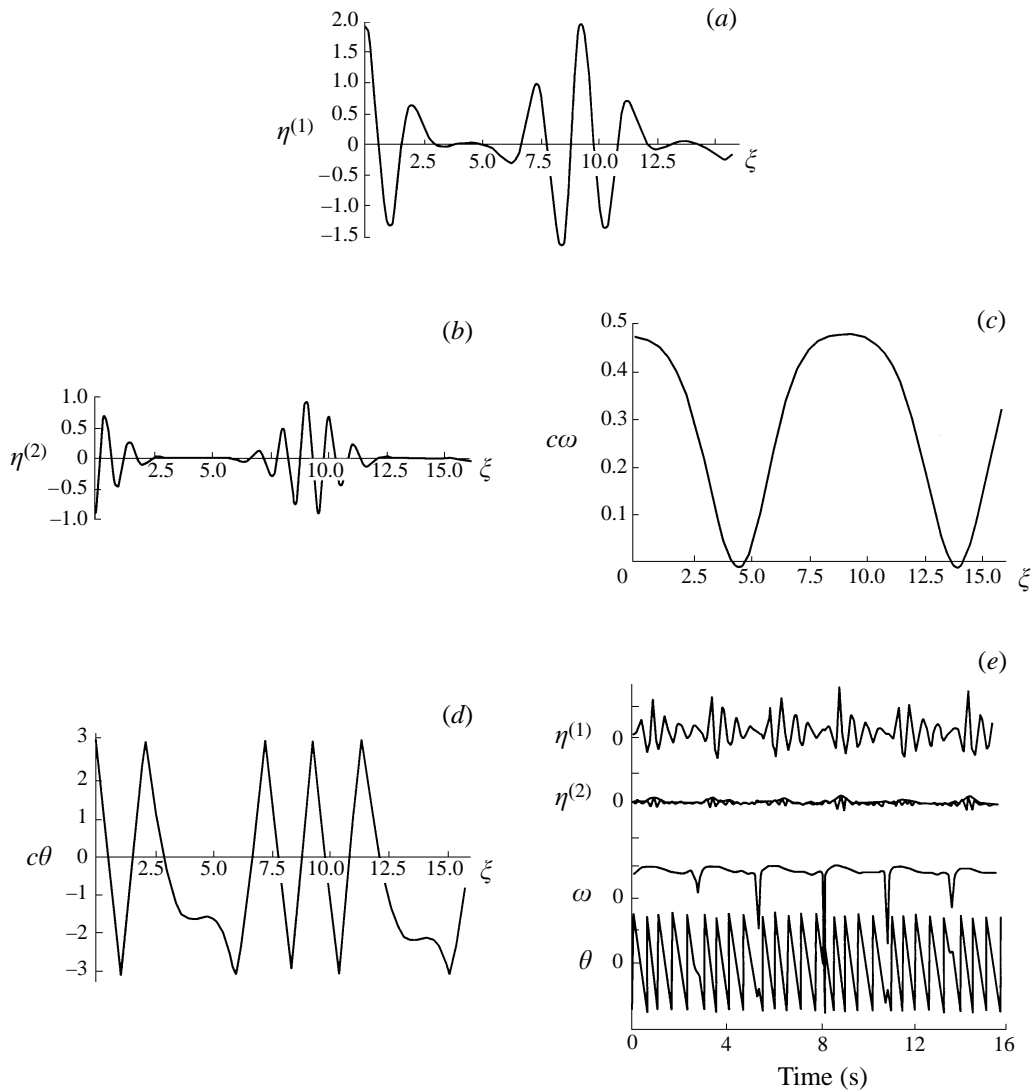


FIGURE 5. As figure 3 but with  $A = 0.35$ ,  $\Delta = -0.50$ ,  $E = 0.20$  and  $\epsilon = 0.15$ . Plots (e) reproduce experimental data by Melville (1983).

increases in the first-harmonic displacement  $\eta^{(1)}$  and a concomitant general growth in the frequency  $c\omega$  (up to the maximum of about  $1/2$ ), while the second-harmonic displacement  $\eta^{(2)}$  has the form of a solitary wave with no ‘pedestal’. Although figure 4(a) does not show clearly a non-zero fundamental harmonic outside the solitary packet due to the numerical procedure, an asymptotically constant wave frequency  $c\omega \approx 0.37$  can be seen in figure 4(c). The principal distinction of this wavepacket from the well-known NSE envelope soliton is just the non-zero wave train at infinity and the varying (elevated for  $A > 0$ ) ‘carrier’ frequency within the perturbed region. (Recall that the wave frequency is fundamentally constant within the NSE soliton.)

According to the previous analysis, we expect a deep wave modulation to ‘smooth’ quasi-periodically the water free surface if the integral cycle approaches the critical

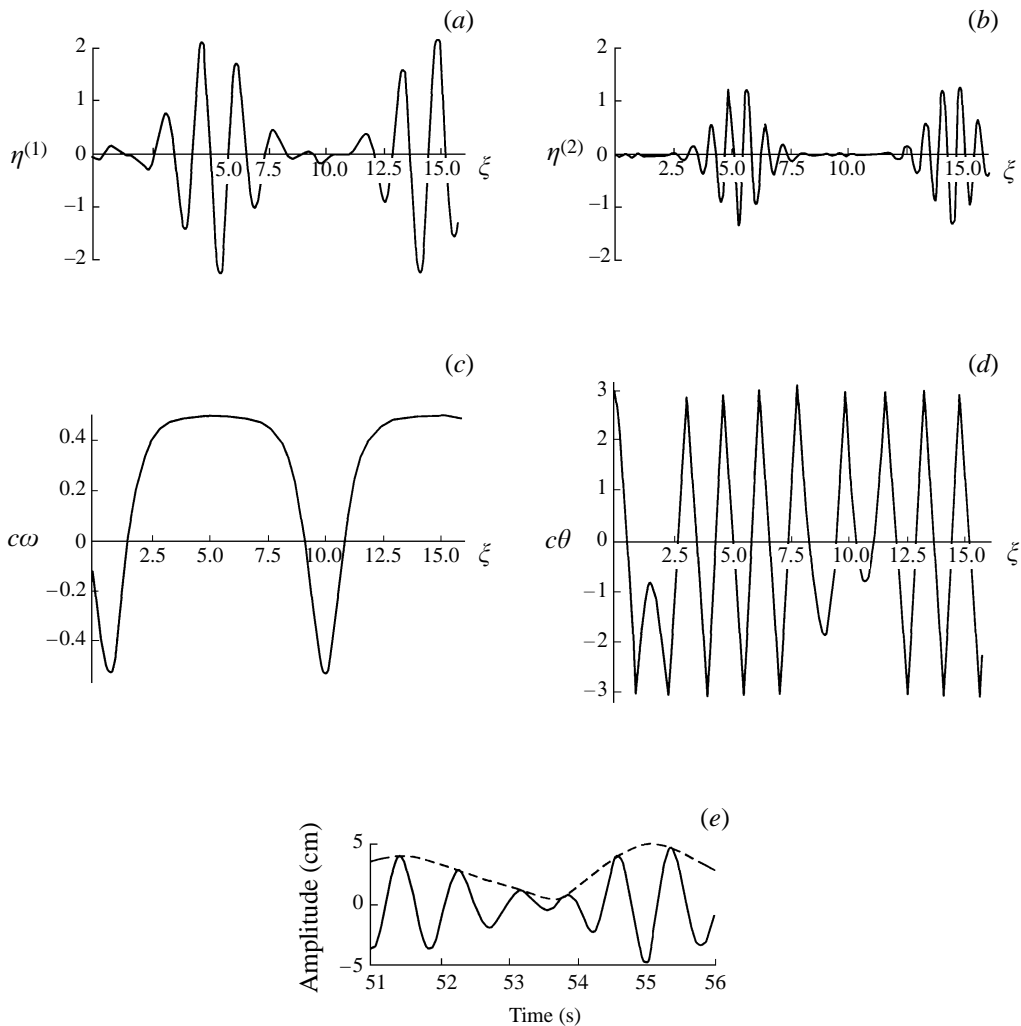


FIGURE 6. As figure 3 but with  $A = 0.10$ ,  $\Delta = -0.50$ ,  $E = 0$  and  $\epsilon = 0.12$ . Graph (e) shows a fragment of experimental data by Chereskin & Mollo-Christensen (1985).

line  $\phi_{0c} = (2A)^{1/2}$  on the phase plane. Such a wave mode is shown in figure 5 for parameters  $A = 0.35$ ,  $\Delta = -0.50$ ,  $E = 0.20$ , and  $\epsilon = 0.15$ . The above smoothing is distinct in the surface profile (figure 5*a, b*), it is especially clear for the second harmonic. A solution of this type has all the main indications of phase reversals observed in the experiments by Melville (1983) and Chereskin & Mollo-Christensen (1985): the wave frequency (figure 5*c*) locally drops from the almost maximum  $c\omega \approx 0.48$  to zero (more correctly, to  $c\omega \approx -0.015$ ), while the phase  $c\theta(\xi)$  (figure 5*d*) has sharp kinks localized exactly at the minimum surface elevations. The phase delays of order  $\pi/2$  take approximately one wave period, during which the wave crests are merging together.

For comparison, some fragments of experimental data by Melville (1983) are reproduced in figure 5(*e*). One sees there a deep modulation regime (at a maximum tank fetch) with the experimental profiles of the two lowest surface harmonics qualitatively similar to those we displayed for the above-specified model parameters. It is also of principal interest that, as the wave displacement is rather small as is the

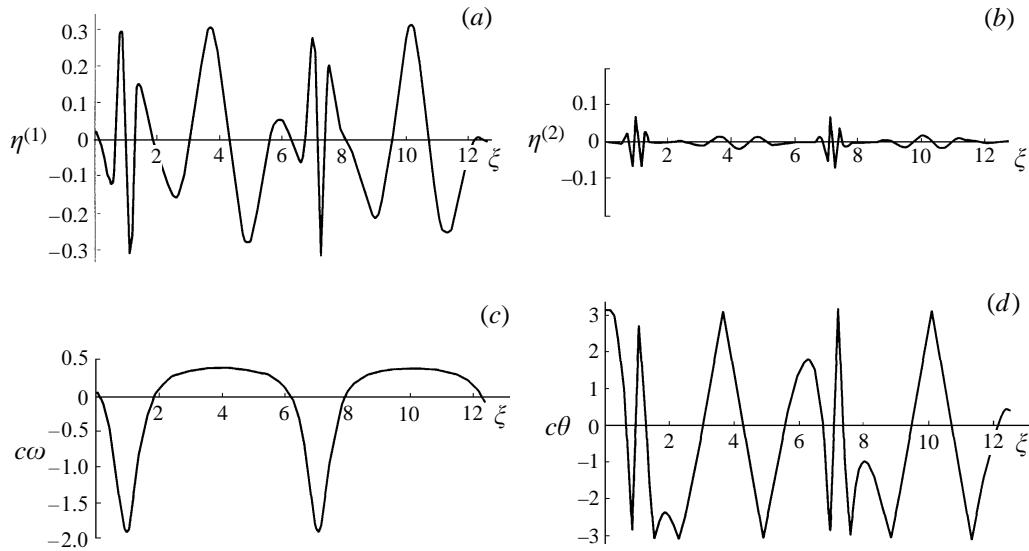


FIGURE 7. As figure 3 but with  $A = 0.07$ ,  $\Delta = 0.50$ ,  $E = 0.075$  and  $\epsilon = 0.15$ .

frequency (for instance, at  $t \approx 3$  s in figure 5e), the experimental phase kinks in deeply modulated waves are also qualitatively well described by the proposed theory (cf. plot *d* of figure 5).

These wave phase reversals become more intense if the potential amplitude  $\phi_0$  within a considerable fraction of the modulation period is sufficiently small compared to the critical value  $(2A)^{1/2}$ . This case is exemplified by curves in figure 6 plotted for the wave action flux  $A = 0.10$ , group detuning  $\Delta = -0.50$ , energy flux  $E = 0$  (no wave sources), and a steepness of  $\epsilon = 0.12$  (almost the same as in figure 5). Figure 6 shows a more effective surface smoothing (curve *a*) and sharper phase kinks (curve *d*). The wave frequency (figure 6c) synchronously with the surface smoothing takes large negative values ( $c\omega \approx -0.54$ ) close in modulus to the maximum positive frequency ( $c\omega \approx 0.49$ ), and the phase (figure 6d) runs in the opposite direction, that is, the phase kinks are  $\pi$  and greater. It is noteworthy that such frequency drops and phase kinks were observed by Melville (1983) (see, for example, the relevant plots at  $t \approx 5$  s and 8 s in figure 5e). The solution in figure 6 also gives evidence for the effects of wave crest loss (pairing) and period doubling observed in experiments by Lake & Yuen (1978), Ramamonjariosa & Mollo-Christensen (1979), Mollo-Christensen & Ramamonjariosa (1982), and Chereskin & Mollo-Christensen (1985) (cf. figures 6a and 6e).

Our theory predicts also, in principle, the existence of solutions where the wave frequency takes even larger negative values. For example, such frequency behaviour is seen in figure 7(c) for  $A = 0.07$ ,  $\Delta = 0.50$ ,  $E = 0.075$ , and  $\epsilon = 0.15$ , plotted together with two surface harmonics and phase (figure 7a, b and d). Large negative frequency spikes cause irregular phase  $c\theta(\xi)$  reversals in the narrow  $\xi$  intervals where, instead of smoothing, a surface roughness arises in the lowest wave harmonics (see figure 7a and b).

In the model, competition between the opposite effects of wave smoothing and roughening can give rise to rather sophisticated motion. Figure 8, where  $A = 0.10$ ,  $\Delta = 0.75$ , and  $E = 0.05$ , shows quite a regular asymmetrical *N*-wave for the first-

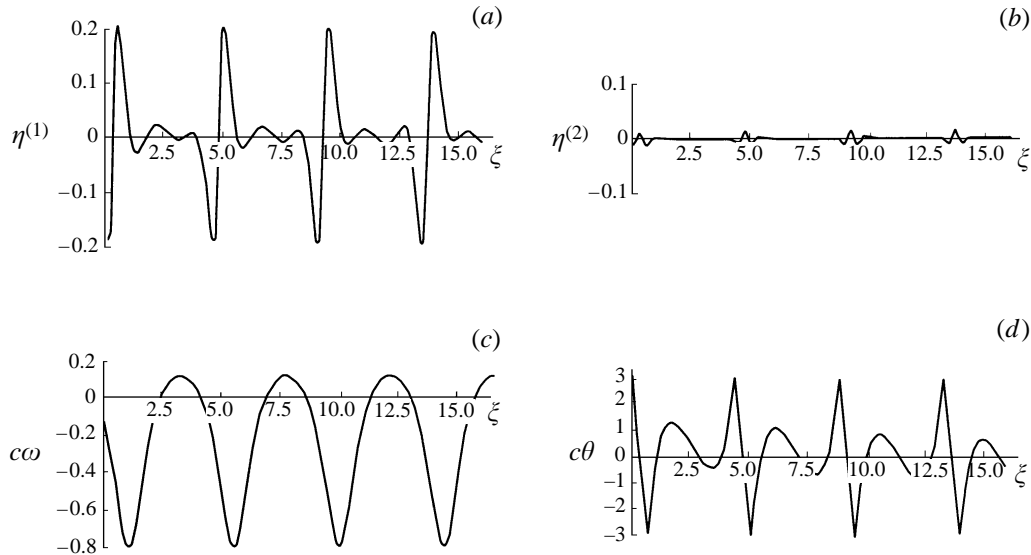


FIGURE 8. As figure 3 but with  $A = 0.10$ ,  $\Delta = 0.75$ ,  $E = 0.05$  and  $\epsilon = 0.15$ .

harmonic surface displacement  $\eta^{(1)}(\xi)$  with an average steepness of  $\epsilon = 0.15$ . The second harmonic  $\eta^{(2)}(\xi)$  reveals only weak periodic splashes, while the wave frequency (figure 8c) is now smoothly and deeply modulated in the  $c\omega$  intervals from approximately 0.12 to a relatively large negative value of about  $-0.8$ . There the phase  $c\theta(\xi)$  undergoes quasi-periodic beats with a reverse in half of the wave modulation period.

#### 4.2. Negative wave action flux

The main properties of travelling wave solutions are noticeably different for a negative wave action flux  $A$  in the laboratory reference frame, when the wave group velocity is lower than the reference one. Seemingly this case corresponds to moderate-modulated surface waves with initial steepness  $\epsilon = 0.23$  observed by Melville (1983): in the experiment the action flux altered its main direction from negative to positive only at the maximum tank length. This is seen just from the change in polarity of frequency deflections and phase variations measured by Melville. Taking these deflections into account and considering formula (4.1) for  $A \leq 0$ , the instantaneous positive shift from the minimum wave frequency  $\omega_{\min} = (2c)^{-1}$  proves to be inversely proportional to the potential amplitude squared. Thus, as the nonlinear effects grow quasi-stationarily at a negative action flux, some average frequency downshift should be observed in moderate-modulated travelling surface waves.

At noticeable wave potential amplitudes,  $\phi_0 \gg (2A)^{1/2}$ , the frequency falls, as the amplitude grows: these parameters are modulated in antiphase in contrast to the previous cases with  $A > 0$ . The free-surface profiles of the first  $\eta^{(1)}(\xi)$  and the second  $\eta^{(2)}(\xi)$  wave harmonics are shown in figure 9 for the negative wave action flux  $A = -0.10$  at  $\Delta = -0.50$ ,  $E = 0$  (no radiating sources), and  $\epsilon = 0.15$ . One sees this type of solution to correspond well to the nonlinear wavepacket propagation with antiphase modulation of the packet amplitude and frequency, observed on relatively short wave fetches by Melville (1983) and Chereskin & Mollo-Christensen (1985). The wavepacket frequency  $c\omega(\xi)$  and phase  $c\theta(\xi)$  are quite regularly but deeply modulated in this example.

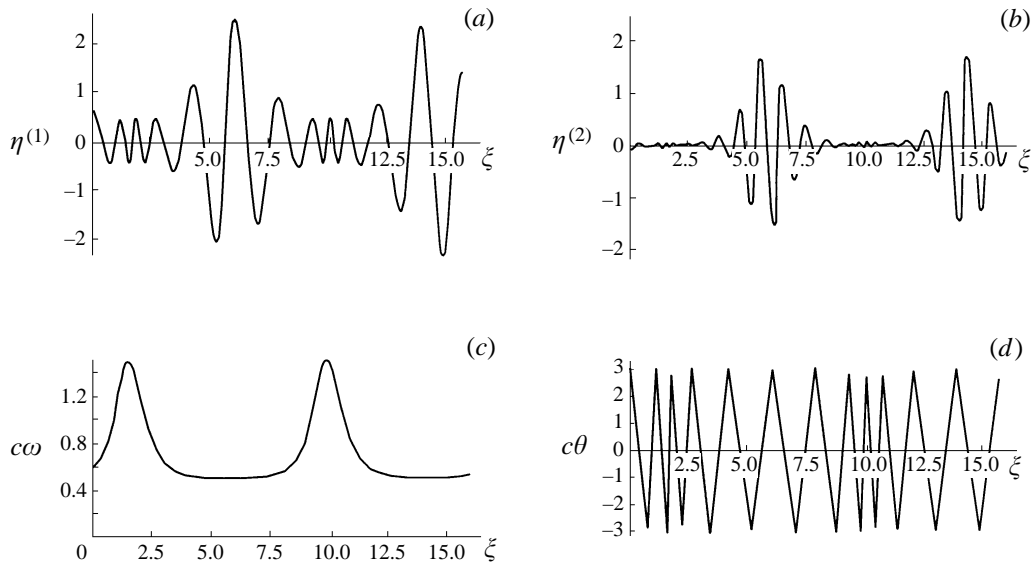


FIGURE 9. As figure 3 but with  $A = -0.10$ ,  $\Delta = -0.50$ ,  $E = 0$  and  $\epsilon = 0.15$ .

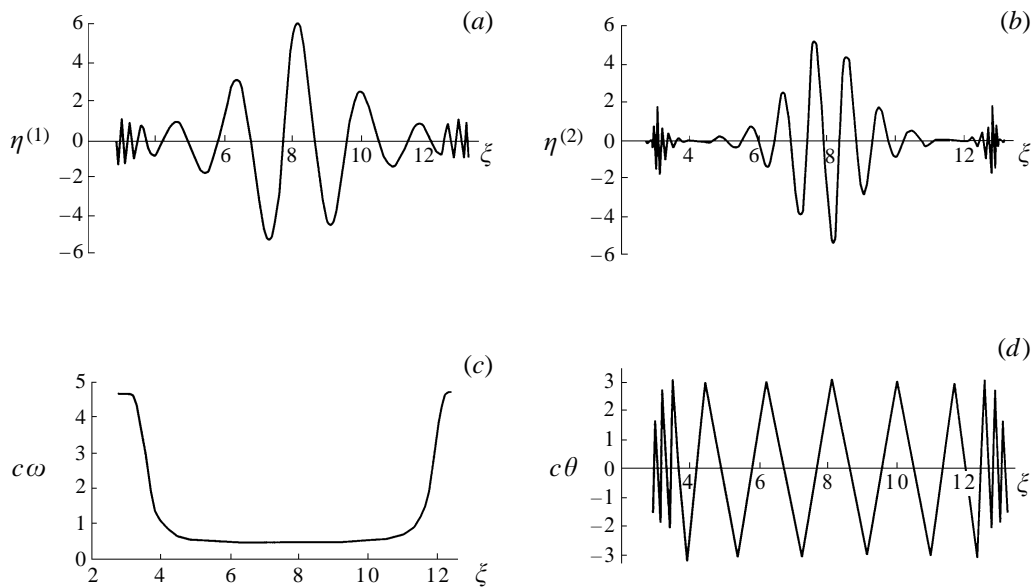


FIGURE 10. As figure 3 but with  $A = -0.30$ ,  $\Delta = 0.30$ ,  $E = 0.375$  and  $\epsilon = 0.15$ .

For negative action flux  $A < 0$ , the solitary wavepackets can also ride on a permanent asymptotically uniform train travelling from infinity, that corresponds to a cyclic part of the type III trajectory in figure 1. This mode is illustrated by graphs in figure 10 plotted for  $A = -0.30$ ,  $\Delta = 0.30$ ,  $E = 0.375$ , and  $\epsilon = 0.15$ . The solitary surface wave is observed as in the first harmonic  $\eta^{(1)}$ , as in the second one  $\eta^{(2)}$ , the former riding on a permanent train of constant amplitude. In figure 10, the frequency sharply drops from a large value  $c\omega \approx 4.7$  to the minimum  $c\omega \approx 0.5$ , being virtually unchanged inside the solitary packet, and then restores fast to an asymptotic level. The wave

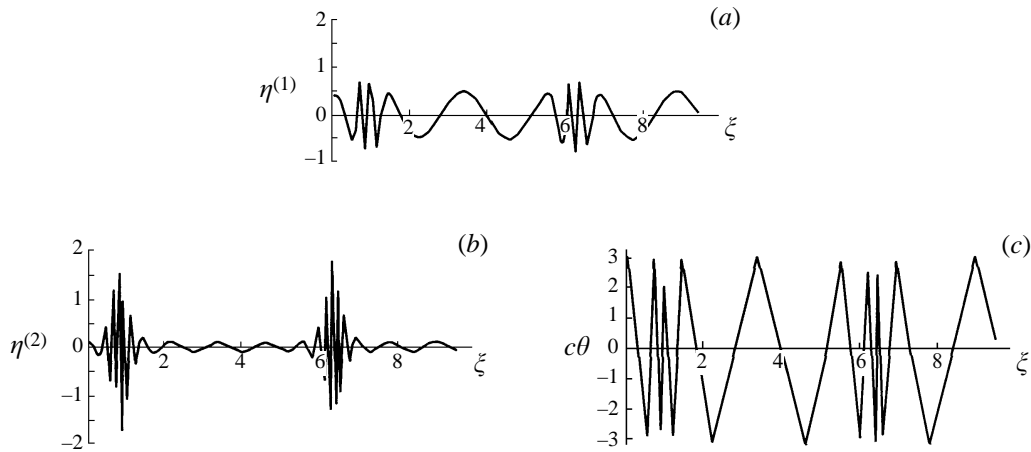


FIGURE 11. As figure 3 but with  $A = -0.09$ ,  $\Delta = -0.50$ ,  $E = 0.12$  and  $\epsilon = 0.25$ ; plot (c) represents the wave phase  $c\theta(\xi)$ .

phase  $c\theta(\xi)$  is modulated in the same manner, being retarded and virtually uniform within the packet.

Again with negative group detuning,  $A < 0$ , and a stationary source of the wave energy flux  $E > 0$  at  $\xi = -\infty$ , a pure frequency-modulated surface wave can be observed in the nonlinear system. For example, such a wave is shown in figure 11 for  $A = -0.09$ ,  $\Delta = 0.50$ ,  $E = 0.12$ , and  $\epsilon = 0.25$ . In this case, a deeply modulated frequency  $c\omega(\xi)$  acts upon both the wave phase  $c\theta(\xi)$  and the fundamental-harmonic elevation  $\eta^{(1)}(\xi)$ , the latter having merely negligible amplitude modulation. However, the second-harmonic displacement  $\eta^{(2)}(\xi)$  presents a periodic sequence of comparatively intense short pulses.

## 5. Concluding remarks

We have analysed various types of permanent envelopes travelling on the surface of deep water, which can be treated as solutions to the equations of the third-order approximation in wave steepness, assuming the wavenumber and frequency variations are not small. The wave motion examples and analysis have demonstrated the main features of these new solutions, including their difference from and reduction to the relevant NSE solutions. Some important nonlinear modulation effects, such as negative frequencies, phase kinks, crest pairing, etc., often observed experimentally at long-fetch propagation of finite-amplitude surface wave trains, are reproduced by the proposed theory. This gives the possibility to design experiments to verify other predictions of the model, especially those concerning the existence of solitary wavepackets with changed frequency, riding on a permanent wave background and containing not many (e.g. five, as in figure 10a) oscillations. The observation of various deeply modulated wave motions predicted in this paper is of general interest. The simply scaled model free parameters can facilitate the choice of dynamic and kinematic wave characteristics appropriate for a relevant laboratory experiment as well as the search for optimum conditions for the field wave measurements.

It is noteworthy that the theory presented, though qualitatively describing the specific modulation of travelling surface waves, can be improved by non-stationary solutions to interpret correctly the average frequency downshift in moderate-modulated waves and by the introduction of (even small) viscosity for a better comparison



with available experimental data. Another important problem is to investigate the stability of stationary wave solutions found in the paper. The effect of higher-order approximations on these solutions should be also evaluated. Besides, the impact of wave sources can be an object of special study since these change substantially the wave motion modelled. Due to the short-scale roughness arising in certain ranges of wave parameters, it would be also useful to take capillary effects into account.

The work was supported by the Russian Foundation for Basic Research under Project Code 96-02-16682a.

## REFERENCES

- AKYLAS, T. R. 1989 Higher-order modulation effects on solitary wave envelopes in deep water. *J. Fluid Mech.* **198**, 387–397.
- AKYLAS, T. R. 1991 Higher-order modulation effects on solitary wave envelopes in deep water. Part 2. Multi-soliton envelopes. *J. Fluid Mech.* **224**, 417–428.
- BENJAMIN, T. B. & FEIR, J. E. 1967 The disintegration of wave trains on deep water. Part 1. Theory. *J. Fluid Mech.* **27**, 417–430.
- CHERESKIN, T. & MOLLO-CHRISTENSEN, E. 1985 Modulational development of nonlinear gravity-wave groups. *J. Fluid Mech.* **154**, 337–365.
- CHU, V. H. & MEI, C. C. 1970 On slowly-varying Stokes waves. *J. Fluid Mech.* **41**, 873–877.
- CHU, V. H. & MEI, C. C. 1971 The nonlinear evolution of Stokes waves in deep water. *J. Fluid Mech.* **47**, 337–351.
- DYSTHE, K. B. 1979 Note on a modification to nonlinear Schrödinger equation for application to deep water waves. *Proc. R. Soc. Lond. A* **369**, 105–114.
- FEIR, J. E. 1967 Discussion: some results from wave pulse experiments. *Proc. R. Soc. Lond. A* **299**, 54–56.
- GROMOV, E. M. & TALANOV, V. I. 1996 Higher order approximations of the dispersion theory for nonlinear waves in homogeneous and inhomogeneous media. *Bull. Russ. Acad. Sci. Phys.* **60**, 1836–1848.
- HARA, T. & MEI, C. C. 1991 Frequency downshift in narrow-banded surface waves under the influence of wind. *J. Fluid Mech.* **230**, 429–477.
- HARA, T. & MEI, C. C. 1994 Wind effects on the nonlinear evolution of slowly varying gravity-capillary waves. *J. Fluid Mech.* **267**, 221–250.
- HUANG, N. E., LONG, S. R. & SHEN, Z. 1996 The mechanism for frequency downshift in nonlinear wave evolution. *Adv. Appl. Mech.* **32**, 59–117.
- KATO, Y. & OIKAWA, M. 1995 Wave number downshift in modulated wavetrain through a nonlinear damping effect. *J. Phys. Soc. Japan* **64**, 4660–4669.
- LAKE, B. M. & YUEN, H. C. 1978 A new model for nonlinear wind waves. Part 1. Physical model and experimental evidence. *J. Fluid Mech.* **88**, 33–62.
- LO, Y. & MEI, C. C. 1985 A numerical study of water-wave modulation based on a higher-order Schrödinger equation. *J. Fluid Mech.* **150**, 395–416.
- LO, Y. & MEI, C. C. 1987 Slow evolution of nonlinear deep water waves in two horizontal directions: a numerical study. *Wave Motion* **9**, 245–259.
- MELVILLE, W. 1983 Wave modulation and breakdown. *J. Fluid Mech.* **128**, 489–506.
- MOLLO-CHRISTENSEN, E. & RAMAMONJARISOA, A. R. 1982 Subharmonic transitions and group formation in a wind wave field. *J. Geophys. Res.* **87**, 5699–5717.
- RAMAMONJARISOA, A. R. & MOLLO-CHRISTENSEN, E. 1979 Modulation characteristics of sea surface waves. *J. Geophys. Res.* **84**, 7769–7775.
- ROSKES, G. 1976 Comments on ‘Nonlinear deep water waves: theory and experiment’. *Phys. Fluids* **19**, 766.
- STANSBERG, G. T. 1995 Spatially developing instabilities observed in experimental bichromatic wave trains. In *26th IAHR Congress (HYDRA 2000)* (ed. A. G. Grass), vol. 3, pp. 180–185. Thomas Telford.
- STOKES, G. G. 1849 On the theory of oscillatory waves. *Trans. Camb. Phil. Soc.* **8**, 441–455.

- SU, M. Y. 1982 Evolution of groups of gravity waves with moderate to high steepness. *Phys. Fluids* **25**, 2167–2174.
- TOMITA, H. 1986 On nonlinear sea waves and the induced mean flow. *J. Ocean. Soc. Japan* **42**, 153–160.
- UCHIYAMA, Y. & KAWAHARA, T. 1994 A possible mechanism for frequency down-shift in nonlinear wave modulation. *Wave Motion* **20**, 99–110.
- WHITHAM, G. B. 1974 *Linear and Nonlinear Waves*. Wiley.
- YUEN, H. & LAKE, B. 1975 Nonlinear deep water waves. Theory and experiment. *Phys. Fluids* **18**, 956–960.
- ZAKHAROV, V. E. 1968 Stability of periodic waves of finite amplitude on the surface of a deep fluid. *Sov. Phys. J. Appl. Mech. Tech. Phys.* No. 2, 190–194.
- ZAKHAROV, V. E. & SHABAT, A. B. 1972 Exact theory of two-dimensional self-focusing and one-dimensional self-modulation of waves in nonlinear media. *Sov. Phys.-JETP* **34**, 62–69.